Failure diagnosis on photovoltaic modules using visual inspection, thermography, electroluminescence and I-V technique

Conference Paper · September 2019

DOI: 10.4229/eupvsec20192019-4av.2.20

A. Moretón
Universidad de Valladolid

Víctor Alonso Gómez
Universidad de Valladolid

Luis Hernández-Callejo
Universidad de Valladolid

Jose Ignacio Morales Aragones
University of Zaragoza

FAILURE DIAGNOSIS ON PHOTOVOLTAIC MODULES USING THERMOGRAPHY, ELECTROLUMINESCENCE, RGB AND I-V TECHNIQUES

Sara Gallardo-Saavedra[1*], Ángel Moretón-Fernández[2], Marta María Jiménez-Martín[2], Víctor Alonso-Gómez[1], Luis Hernández-Callejo1, Óscar Martínez-Sacristán[2], Miguel Ángel González-Rebollo[2] and José Ignacio Morales-Aragonés[1].

[1]Universidad de Valladolid (UVa), School of Forestry, Agronomic and Bioenergy Industry Engineering (EIFAB), Department of Agricultural and Forestry Engineering, Campus Duques de Soria, 42004 Soria (Spain);
[*]sara.gallardo@uva.es
[2]GdS-Optronlab, Dept. Física de la Materia Condensada, Universidad de Valladolid (UVa), Paseo de Belén, 19, 47011 Valladolid (Spain)

ABSTRACT: Different techniques can be used to detect and quantify PV modules anomalies, as visual inspections, electrical tests like the I-V curve test, infrared thermography (IRT) or electroluminescence (EL). PV plants operators usually apply only one or two of them within the Operation and Maintenance (O&M) activities. Additionally, researchers usually studied them separately. However, these methods provide complementary results, glimpsing interesting information about the PV site state. The main strength of the research performed is the simultaneous study of all these inspection techniques, studying the correlation between them. Results confirm that, EL and IRT under current injection on modules are closely correlated, while IRT under normal operation (sun exposure) reveals complementary information not detected in EL but existing in the visible spectrum. In conclusion, it is advisable using as many techniques as possible to characterize the actual state of the module and to explain its I-V curve.

Keywords: photovoltaic inspection, faults diagnosis, photovoltaic thermography, photovoltaic electroluminescence, IV curve.

1 INTRODUCTION

Increasing photovoltaic (PV) modules reliability and life time is the most important factor for the energy efficiency in PV systems, reducing costs and uncertainties. PV modules are the main component within a PV system, as they convert sunlight into electricity using semiconducting materials, through the well-known photovoltaic effect. The aim of continuous development of PV technology is not only to improve the efficiency of the cells but also to reduce production cost of the modules, making it more feasible for various applications [1]. However, the production cost reduction should not affect the modules quality and being able to detect, to identify and to quantify the severity of defects that appear within modules is essential to constitute a reliable, efficient and safety system, avoiding energy losses, mismatches and safety issues.

Typically, failures can be divided into three categories: infant-failures, midlife-failures, and wear-out-failures. The bathtub curve is widely used in reliability engineering, describing a form of the hazard function. A PV module failure is an effect that degrades the module power which is not reversed by normal operation or creates a safety issue. Different kind of failures that appear in PV modules are: delamination, back sheet adhesion loss, junction box failure, frame breakage, EVA discoloration, cell cracks, snail tracks, burn marks, potential induced degradation (PID), disconnected cells or defect bypass diode [2].

Different techniques can be used to detect and quantify PV modules anomalies. Traditionally, faulty modules or cells within a PV plant have been located by applying visual inspections, electrical tests like the I-V curve test or manual infrared thermography (IRT). Visual inspection is efficient, cheap and quick, but only reveals some of the failures. For example, typical failures found during visual inspections according to IEC 61215 are bubbles, delamination, yellowing and browning in the front of the module, broken cells, cracked cells or discoloured anti reflection, burned or oxidized cells metallization, failures in the frame, delamination, bubbles, scratches or burn in the back of the module, loose, oxidation or corrosion in the junction box and detachment or exposed electrical parts in wires or connectors. I-V curve (current versus voltage curve) provides important information about the electrical performance of the system, and its main parameters. In order to be able to compare results, since it is not always possible to measure the curve in the Standard Test Conditions (STC), it is necessary to apply a translation procedure, which can be used in a certain range from the measured conditions [3]. An accurate I-V curve interpretation gives relevant information about the module failures, revealing degradation, mismatched modules, cracked cells, improper resistance, shadings or bypass diodes malfunction [4]. IRT is a technique that detects heat distribution in an evaluated area. This method measures the characteristics of radiative heat in order to set areas or points with higher or lower heat emissivity, areas that could indicate the presence of a fault. Possible thermographic defects detected in a PV module are: cell hotspot, overheated bypass circuit, junction box, connection or whole module [5]. Later, the huge size of newer PV plants has been responsible of the development of innovative techniques, such as the aerial thermography [6], to enable or optimize maintenance activities. A fourth method to analyse the system condition is electroluminescence (EL), which can be used in manufacturing process, shipped to a lab after unmounting the modules from the site or on the field, with an structure or specific tripod or also by means of EL cameras mounted on UAVs. In this case, the radiative recombination of charge carriers causes light emission in the solar cells, which is captured by an EL camera and the emission intensity serves as an indicator of the healthiness of the solar cell [7]. The high resolution of the EL images enables resolving some defects more precisely than in IR images [8]. Each of these techniques has some advantages and disadvantages, and based on them, PV plants operators usually apply only one or two of these techniques within the Operation and Maintenance (O&M) activities. Additionally, the results provided by each of them are usually studied separately, by different research groups.

However, these methods can provide complementary results, glimpsing interesting information about the PV site state. Sometimes, the complicated situation of having the concurrent presence of different kinds of defects makes it difficult to quantify the impact of each of them on the overall power losses, which can be clarified using different inspection techniques.

The main strength of the research performed is the simultaneous study of all the inspection techniques described in the previous section, studying the correlation between them: visual, I-V curves, IRT and EL. Previous researches usually study each of them separately, for instance EL for the diagnosis of crystalline silicon solar cells [9], characterization of defects using EL [10], EL imaging for automated defect characterization [11], electromagnetic induction excited IRT [12], correlation between defects and string power by means of aerial thermography inspection [13] or experimental impact on the I-V curve of discoloration and cracks [14]. However, it has been proved that results correlation reveal complementary information, improving the faults detection, quantification and diagnosis.

2 MATERIALS AND METHOD

Indoor and outdoor tests have been conducted in the School of Forestry, Agronomic and Bioenergy Industry Engineering (EIFAB) in Soria, Spain. Between the indoor tests, EL has been performed in controlled ambient conditions simultaneously than IRT in the fourth quadrant. For these tests, the University has a temperature and humidity controlled chamber, which is shown in Figure 1.

Figure 1: Temperature and humidity controlled chamber at the EIFAB in Soria, Spain

In this chamber, each module is continuously fed with its short circuit current, using a laboratory source, during 72 hours. EL images are captured with a pco. 1300 camera each 30 minutes with an exposure of 5,000 ms. Thermal images has been captured with a Flir C2 system and a Workswell Wiris Pro camera. This capturing system is presented in Figure 2, in which can be seen the EL camera, the IR camera and the PC which control the acquisition.

Figure 2: EL and IR imaging capturing system used in the temperature and humidity controlled chamber

Outdoor tests include I-V curves, IRT and RGB images in the PV field of the Campus Duques de Soria, University of Valladolid, which can be seen in Figure 3. The thermal camera used outdoor is a Workswell Wiris Pro camera, with a 640x512 pixels resolution, a thermal sensitivity of 0.05ºC and an accuracy of ±2% o ±2°C. Additionally, the camera has a frame rate of 30Hz, is calibrated to be used with two different lenses, 32º y 69º, and includes a Full HD RGB sensor with a resolution of 1920x1080 pixels and x10 zoom. The I-V curves have been traced using an I-V tracer Solar IV HT 1500V.

Figure 3: PV field of the Campus Duques de Soria, University of Valladolid.

The modules tested present different kinds of defects and they are mono and poly crystalline modules from different manufacturers. However, this paper summarizes the results of one of them. Its nominal data is presented in Table 1.

Table 1: Nominal information of the module analysed in this research

Lab Name	Power (W)	Type	Cells	Voc (V)
S-E1	165	Mono	72	43,92
	Vmpp (V)	Isc (A)	Impp (A)	Toll
	35,64	5,23	4,63	±5

3 RESULTS AND DISCUSSION

As it has already been highlighted, the main purpose of this research is to study the information provided by each inspection technique and the relation between them. For each module, it has been performed its IV curve before and after the EL, EL images each 30 min during 72 hours, thermal images of the fourth quadrant each minute during the EL process and thermal images of the second quadrant during the modules operation in the PV field of the Campus Duques de Soria. Additionally, RGB images has been captured before and after each test.

Some relevant results achieved in the research will be discussed along this section. Regarding the PV module S-E1, which main nominal characteristics have been described in the previous section, results show that there is not any significant change between the IV curves shape before and after the EL test. The first and the last EL images of the stack are presented in Figure 4 a) and b), respectively. This means that the continuously fed short circuit current injection during 72 hours does not affect considerably the modules performance. It is important to consider that it has been an EL test to evaluate the modules behaviour during prolonged periods of current feeding them. However, during an ordinary EL test on-site, the modules are exposed during a minimum period of time, just in the moment the EL images are going to be taken. The same module captured with a visual camera is presented in Figure 4, c).

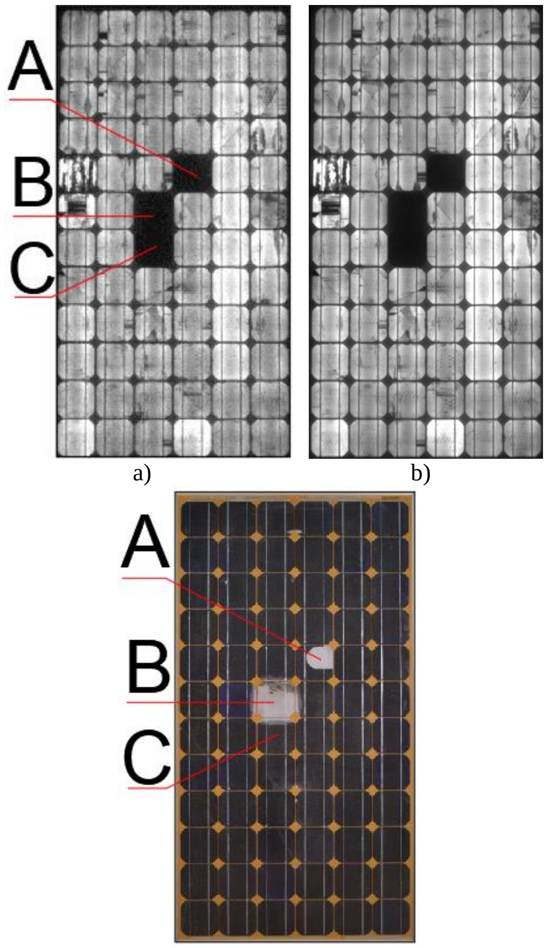

Figure 4: First (a) and last (b) EL images of S-E1 module and its RGB appearance (c).

In this visual image, it can be seen an EVA delamination failure in the cell labelled as A, and a burn area, combined with delamination, in cell B. Apparently, cell C does not present important failures detected visually, but failure B apparently is extended in the upper area of cell C. However, these three cells are inactive, as it can be seen in the EL images, appearing completely black, as they do not emit. Therefore, it can be concluded that these cells are short-circuited, allowing the current passing but not producing energy. Although cell C visually does not present any relevant defect, the failure B has extended affecting likewise cell C. This fact is also revealed in the IV Curve, which can be seen in Figure 5. In this figure are showed two different test performed at different irradiance and temperature conditions and extrapolated to Standard Test Conditions (STC). Its main parameters are compared with the nominal data of the module in Table 2. It can be seen an open circuit voltage (Voc) drop of 3,45V, which correspond with the contribution of the three inactive cells in addition to other partial inactive cells, as it can be seen in the EL images in Figure 4. The short circuit current (Isc) does not significantly fall because the rest of cells are almost fully active (in the sense of cell area working).

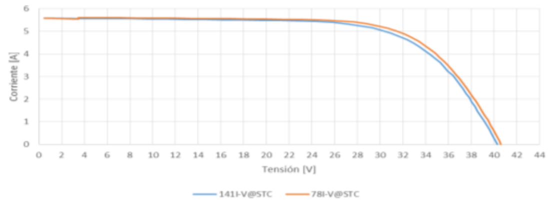

Figure 5: IV Curve of the S-E1 module in STC.

Table 2: Main parameters of the S-E1 module measured (STC) and nominal.

	PMAX (W)	VOC (V)	VMPP (V)	IMPP (A)	ISC (A)
STC	152,52	40,47	30,46	5,01	5,54
Nominal	165,00	43,92	35,64	4,63	5,23

Finally, IRT has also been studied. Results under current injection conditions are showed in Figure 6 and during ordinary production conditions can be seen in Figure 7.

Results presented in Figure 6 show how total inactive cells remains cooler than active areas during the current injection for the EL test. Additionally, it has been observed that when there is an inactive area within a cell partially active, the active area is revealed as an overheated area. Therefore, it can be concluded that thermographic images during the EL tests also gives complementary information. In Figure 7, the module S-E1 is in landscape mounting mode, with its connection box in the right side of the image. The long hotter area in the right part of the module is the reflection of the anemometer post, which can be seen in the RGB image (Figure 7 b). The three Failures A, B, and C that have been analysed during this paper are also revealed in operation, as hot spots whose defects make them work in the second quadrant. However, the delamination that the module present in A and B, produces a change in the material emissivity value with respect the rest of the glass, responsible of covering up the hot spots, as the delaminated areas appear cooler than their actual temperature.

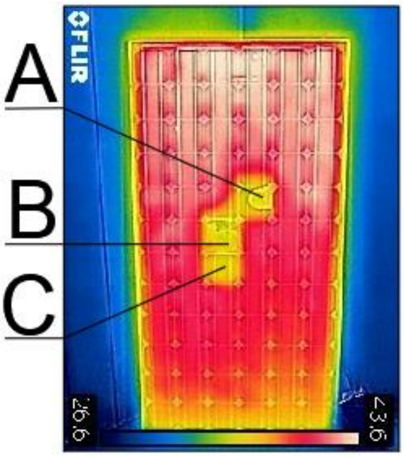

Figure 6: Thermographic image of S-E1 in the fourth quadrant during the EL test.

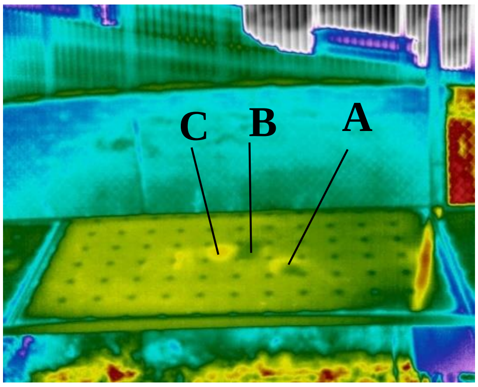

a)

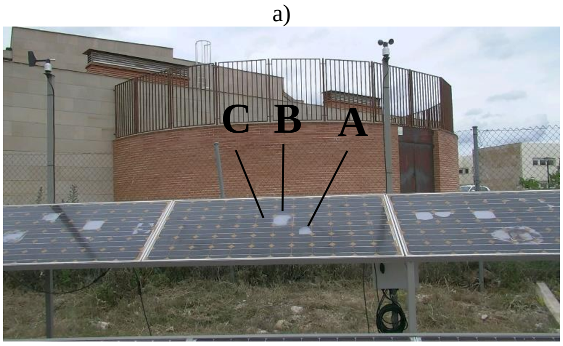

b)

Figure 7: Thermographic (a) and visual (b) images of S-E1 outdoor in ordinary module operation.

4 CONCLUSIONS

The paper presents a simultaneous analysis of different inspection techniques, studying the correlation between them: visual, I-V curves, IRT and EL. Results reveal complementary information between different practises, adding value to individual findings.

Each of the techniques has some advantages and disadvantages. It has been seen that continuously fed short circuit current injection during 72 hours does not affect considerably the modules performance, as EL and RGB images do not reveal important changes in the module. It has been proved how EL images and IRT in the fourth quadrant have high correlation, as total inactive cells remains cooler than active areas during the current injection for the EL test. However, the similarity with IRT during ordinary operation of the modules is not direct, as some active areas appears as hot spots but they can be covering up by delamination, which causes a different emissivity value. Finally, it has been explained how total inactive cells are revealed as a Voc drop in the IV curve, maintaining the curve shape if they are not mixed with other kinds of defects.

ACKNOWLEDGMENT

This work was financed by projects ENE2017-89561-C4-R-3 and RTC-2017-6712-3 of the Spanish Ministry of Science, Innovation and Universities.

REFERENCES

[1] El Chaar L, Lamont LA, El Zein N. Review of photovoltaic technologies. Renew Sustain Energy Rev 2011;15:2165–75. doi:10.1016/j.rser.2011.01.004.
[2] Köntges M, Kurtz S, Packard C, Jahn U, Berger KA, Kato K, et al. Review on Failures of Photovoltaic Modules, Report IEA-PVPS T13-01:2013. 2013.
[3] Bühler AJ, Perin Gasparin F, Krenzinger A. Post-processing data of measured I–V curves of photovoltaic devices. Renew Energy 2014;68:602–10. doi:10.1016/J.RENENE.2014.02.048.
[4] Deviations IT. Solar I-V Curves Interpreting I-V. SolarPro August-September 2014.
[5] Gallardo-Saavedra S, Hernádez-Callejo L, Duque-Pérez Ó. Analysis and characterization of thermographic defects at the PV module level. Rev Fac Ing from Univ Antioquia 2019:1–16.
[6] Gallardo-Saavedra S, Hernández-Callejo L, Duque-Perez O. Technological review of the instrumentation used in aerial thermographic inspection of photovoltaic plants. Renew Sustain Energy Rev 2018;93:566–79. doi:10.1016/j.rser.2018.05.027.
[7] Hallam B, Hamer P, Kim M, Nampalli N, Gorman N, Chen D, et al. Field Inspection of PV Modules: Quantitative Determination of Performance Loss due to Cell Cracks using EL Images. 2017 IEEE 44th Photovolt. Spec. Conf. PVSC 2017, 2017, p. 1858–62. doi:10.1109/PVSC.2017.8366560.
[8] Jahn U, Herz M, Köntges M, Parlevliet D, Paggi M, Tsanakas I, et al. Review on Infrared and Electroluminescence Imaging for PV Field Applications. 2018.
[9] Fuyuki T, Kitiyanan A. Photographic diagnosis of crystalline silicon solar cells utilizing electroluminescence. Appl Phys A Mater Sci Process 2009;96:189–96. doi:10.1007/s00339-008-4986-0.
[10] Kendig D, Alers GB, Shakouri A. Characterization of defects in photovoltaics using thermoreflectance and electroluminescence imaging. Conf Rec IEEE Photovolt Spec Conf 2010:1733–6. doi:10.1109/PVSC.2010.5616126.
[11] Bazzoli M, Silverman TJ, Goddard LL. Low-cost electroluminescence imaging for automated defect characterization in photovoltaic modules. Photonics Conference (IPC), IEEE. 2017:481–2.
[12] He Y, Du B, Huang S. Non-contact Electromagnetic Induction Excited Infrared Thermography for Photovoltaic Cells and Modules Inspection. IEEE

Trans Ind Informatics 2018;14:5585–93. doi:10.1109/TII.2018.2822272.
[13] Dalsass M, Scheuerpflug H, Fecher FW, Buerhop-Lutz C, Camus C, Brabec CJ. Correlation between the generated string powers of a photovoltaic power plant and module defects detected by aerial thermography. 2017 IEEE 44th Photovolt Spec Conf PVSC 2017 2018:1–6. doi:10.1109/PVSC.2017.8366737.
[14] Sarikh S, Raoufi M, Bennouna A, Benlarabi A, Ikken B. Photovoltaic Discoloration and Cracks: Experimental Impact on the I-V Curve Degradation, Springer, Singapore; 2019, p. 609–16. doi:10.1007/978-981-13-1405-6_69.